Diurnal and nocturnal mosquitoes escape looming threats using distinct flight strategies

Current Biology

Cribellier, Antoine; Straw, Andrew D.; Spitzen, Jeroen; Pieters, Remco P.M.; Leeuwen, Johan L. et al

https://doi.org/10.1016/j.cub.2022.01.036

Article

Current Biology

Diurnal and nocturnal mosquitoes escape looming threats using distinct flight strategies

Highlights

- Escaping mosquitoes rely both on their baseline unpredictability and maneuverability
- Baseline flight unpredictability has a major effect on escape performances
- Night-active *Anopheles* mosquitoes exhibit maximum escape performance in the dark
- Day-active *Aedes* shows enhanced escape performance and maneuverability in daylight

Authors

Antoine Cribellier, Andrew D. Straw, Jeroen Spitzen, Remco P.M. Pieters, Johan L. van Leeuwen, Florian T. Muijres

Correspondence

florian.muijres@wur.nl

In brief

Cribellier et al. study how diurnal and nocturnal mosquitoes evade a looming threat by tracking 10,000 evasive maneuvers of *Anopheles* and *Aedes* mosquitoes in various light conditions. They find that both species exhibit enhanced escape performance in their respective natural light conditions, which they achieve using distinct flight strategies.

Cribellier et al., 2022, Current Biology *32*, 1232–1246
March 28, 2022
https://doi.org/10.1016/j.cub.2022.01.036

CellPress

CellPress

Current Biology

Article

Diurnal and nocturnal mosquitoes escape looming threats using distinct flight strategies

Antoine Cribellier,[1,4] Andrew D. Straw,[2,5] Jeroen Spitzen,[3,6] Remco P.M. Pieters,[1] Johan L. van Leeuwen,[1] and Florian T. Muijres[1,7,*]

[1]Experimental Zoology Group, Wageningen University, De Elst 1, 6708 WD, Wageningen, the Netherlands
[2]Institute of Biology I and Bernstein Center Freiburg, University of Freiburg, Hauptstraße 1, 79104 Freiburg, Germany
[3]Laboratory of Entomology, Wageningen University, Droevendaalsesteeg 1, 6708 PB, Wageningen, the Netherlands
[4]Twitter: @AntCribellier
[5]Twitter: @strawlab
[6]Twitter: @Anopheline
[7]Lead contact
*Correspondence: florian.muijres@wur.nl
https://doi.org/10.1016/j.cub.2022.01.036

SUMMARY

Flying insects have evolved the ability to evade looming objects, such as predators and swatting hands. This is particularly relevant for blood-feeding insects, such as mosquitoes that routinely need to evade the defensive actions of their blood hosts. To minimize the chance of being swatted, a mosquito can use two distinct strategies—continuously exhibiting an unpredictable flight path or maximizing its escape maneuverability. We studied how baseline flight unpredictability and escape maneuverability affect the escape performance of day-active and night-active mosquitoes (*Aedes aegypti* and *Anopheles coluzzii*, respectively). We used a multi-camera high-speed videography system to track how freely flying mosquitoes respond to an event-triggered rapidly approaching mechanical swatter, in four different light conditions ranging from pitch darkness to overcast daylight. Results show that both species exhibit enhanced escape performance in their natural blood-feeding light condition (daylight for *Aedes* and dark for *Anopheles*). To achieve this, they show strikingly different behaviors. The enhanced escape performance of *Anopheles* at night is explained by their increased baseline unpredictable erratic flight behavior, whereas the increased escape performance of *Aedes* in overcast daylight is due to their enhanced escape maneuvers. This shows that both day and night-active mosquitoes modify their flight behavior in response to light intensity such that their escape performance is maximum in their natural blood-feeding light conditions, when these defensive actions by their blood hosts occur most. Because *Aedes* and *Anopheles* mosquitoes are major vectors of several deadly human diseases, this knowledge can be used to optimize vector control methods for these specific species.

INTRODUCTION

To get a blood meal for egg development, hematophagous female mosquitoes need to interact with blood hosts, such as humans, cattle, or birds. Because mosquitoes are both a nuisance to hosts and vectors of diseases, such as malaria and yellow fever, these hosts can exhibit defensive behaviors, such as swatting, pecking, or tail swishing, to kill, push away, or discourage the mosquito.[1–6] Additionally, flying mosquitoes can be attacked by predators such as dragonflies, birds, or bats.[7–9] Many of these animals exhibit advanced attacking strategies, such as minimizing changes in the visual angle of their target, either to follow or intercept their prey.[10] Dragonflies approach their prey from below[11,12] and camouflage into immobile distant objects during the attack.[13] Bats use a comparable motion-camouflage strategy.[14] However, it is not known if mosquitoes exhibit counter-strategies against the attacks of predators or blood hosts.

To successfully escape from looming threats produced by defensive blood hosts or predators, a flying mosquito might rely on three behavioral components: first, its baseline protean movement; second, its systematic evasive maneuvers; and lastly, the protean aspect of its evasive maneuvers. Protean behavior is defined as resembling that of Proteus, thus behaving variably or irregularly. In this context, a protean behavior would be an erratic flight behavior that prevents the predator or host from predicting accurately the position of the flying mosquito.[15,16] Although protean behaviors are a widespread anti-predator strategy, their effect on escape performance has been studied very little.[15,17] If exhibited continuously or in risky situations (e.g., while host-seeking), such protean behavior could be seen as an insurance against attacks that might be difficult to detect or to avoid[15] and, if exhibited during evasive maneuvers, protean movements can increase the chance of success of the maneuvers by making them less predictable.

To avoid a threat, mosquitoes might also exhibit systematic evasive maneuvers, such as the ones observed in other insects and birds when attacked by visually looming targets.[18–20] Such stimulus-triggered maneuvers are usually directed away from

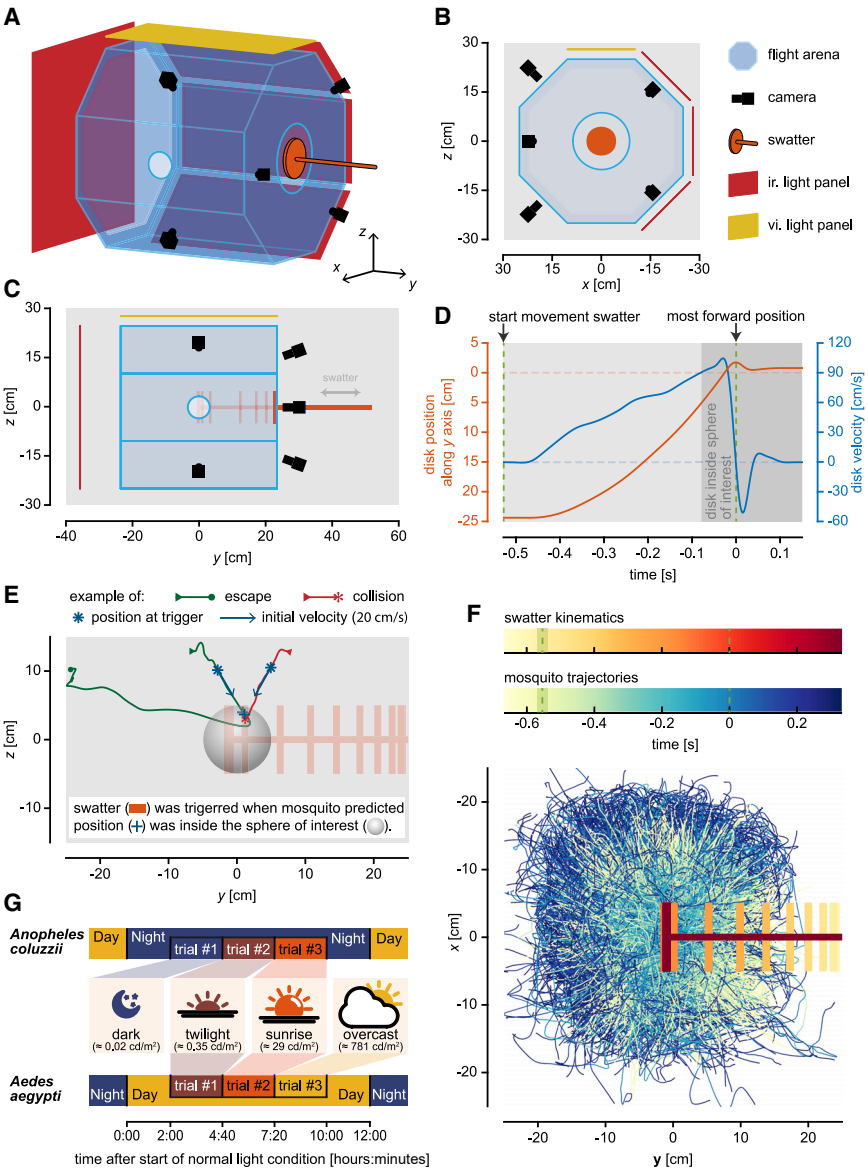

Figure 1. Experimental setup, tested conditions and recorded flight trajectories

(A–C) Schematic views of flight arena with the five-camera real-time tracking system and the event-triggered mechanical swatter.

(D and E) The swatter was triggered when a mosquito was predicted to fly into a virtual sphere in the middle of the flight arena. (D) Attack kinematics of the mechanical swatter. (E) Examples of two flight tracks that triggered the swatter and resulted in an escape or a collision (green and red, respectively). Examples of a collision, a miss, and an escape can be seen in the Videos S1, S2, and S3, respectively.

(F) Temporal dynamics of the positions of the swatter and of all recorded mosquito flight trajectories.

(G) During each experimental day, mosquitoes flew in three semi-randomly changed light conditions during their active period of the day (night-time and day-time for *Anopheles* and *Aedes*, respectively). Because *Anopheles* and *Aedes* fly very little in daylight and in the dark, respectively, we did not perform experiments in these conditions.

the danger,[18] or toward safety zones at the flank of the attacking animal.[21] Similar to horse flies, female mosquitoes make fast upward maneuvers after encountering specific host cues or airflow conditions,[22–25] suggesting that these maneuvers might be examples of such evasive maneuvers.

To detect a threat, a mosquito may rely on its sophisticated sensory system. Mosquitoes can detect CO_2, body odors, visual cues, and heat generated by a nearby blood host.[26–28] However, among these sensory cues, only looming visual cues could be used to detect an incoming attack. It is also possible that mosquitoes use their mechanoreceptors (antennas and sensory hairs) to detect and react to the air movements generated by an attacker.[29] Such an airflow-mediated response has already been described in large ground-dwelling insects, such as praying mantis and crickets,[30–32] and could be an alternative to vision-mediated responses in low light intensities. This would be particularly relevant for night-active mosquitoes. Additionally, it is possible that escaping mosquitoes are simply swept by the airflow produced by an attacker. However, such passive usage of attacker-induced air gusts remains to be described in the scientific literature.

There is also a lack of knowledge about how environmental conditions affect the escape performances and strategies of insects. Because vision allows an animal to detect a threat from a relatively large distance, the light condition is probably the most important factor that can influence the success rate of escapes.[33] Therefore, we expect that diurnal mosquitoes will rely principally on vision to detect a threat in bright light conditions. In contrast, nocturnal mosquitoes flying in pitch darkness cannot use vision to detect a threat; thus, they may rely principally on the detection of the attacker-induced air gust, or potentially a passive use of it. Alternatively, these night-active mosquitoes might rely more on distinct protean behavior to increase their escape performance. Comparing escape performances of day-active and night-active mosquitoes in various light conditions should inform us on how these differences in natural light conditions influence escape strategies.

We studied the escape dynamics of female mosquitoes being attacked by a looming object. For that, we used a real-time videography-based mosquito tracking system to record the 3D movements of mosquitoes flying freely in a flight arena (Figures 1A–1C). Based on the position and velocity of the flying mosquito, we automatically triggered a 10 cm diameter mechanical swatter to simulate the attack of a human hand, generating both visual and air movement cues. By varying the light intensity inside the flight arena from dark night-time conditions to overcast daylight conditions, we studied the effect of light conditions

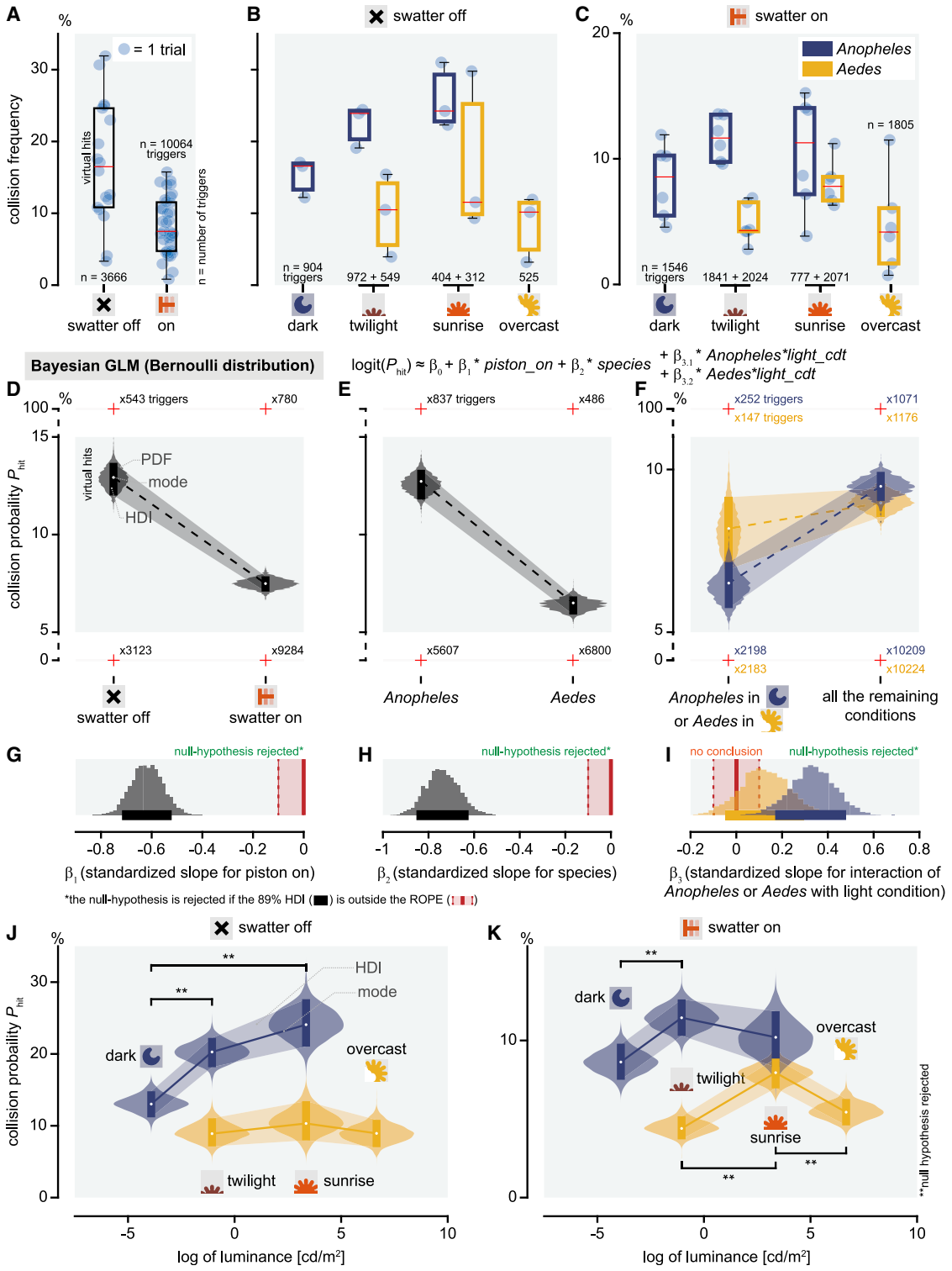

Figure 2. Collision probabilities of mosquitoes with the mechanical and simulated swatter (swatter on and off, respectively)

(A–C) Collision frequency, defined as the number of collisions per number of triggers, in each tested condition. Standard box-and-whisker plots are shown. For the control experiments with the swatter turned off, we estimated virtual collisions by simulating the movement of a virtual swatter. Because *Anopheles* and *Aedes* fly very little in daylight and in the dark, respectively, we did not perform experiments in these conditions. Boxplots of various escape performance parameters can be found in Figure S4.

(D–F) Results (violin plots) of the Bayesian-GLM that modeled the mean collision probability as a function of experimental conditions (including swatter on and off). Each panel is a slice plot showing only the effect of one predictor with the other predictors set at their mean values. Distributions are estimates of the mean

(legend continued on next page)

on the escape performance of the mosquito. Finally, we performed this study with both night-active mosquitoes (*Anopheles coluzzii*) and day-active *Aedes aegypti*. This allowed us to test how escape performance differed between species that are specialized in blood-feeding in dark night conditions and daylight conditions, respectively.

The mosquito species studied here have a strong innate preference for human hosts[34] and are two major vectors of a range of human diseases, including malaria, yellow fever, Zika, and dengue. Therefore, our results can be used to optimize existing or develop new species-specific mosquito trapping systems.

RESULTS

We recorded the flight behavior of mosquitoes during 54 experimental trials of 160 min in length each (144 h in total). These trials consisted of 18 controls during which the mechanical swatter was turned off and 36 trials with the mechanical swatter turned on. Half of these trials were performed on *Anopheles* mosquitoes in the dark, twilight, and sunrise light conditions, and the other half were performed on *Aedes* in the twilight, sunrise, and overcast conditions.

We recorded and analyzed a total of 13,730 mosquito flight tracks (Figure 1F). This included 10,064 flight tracks in experiments with the swatter activated and triggered and 3,666 flight tracks in control experiments. During these control experiments, the swatter was turned off, and we instead simulated an in-silico virtual swatter attack. If the reconstructed flight track of the mosquito crossed the path of this virtual swatter, then the mosquito was classified as virtually hit. These virtual hits occurred in 15% of the 3,666 cases, whereas with the swatter activated, 8% of the approaching mosquitoes were hit (Figure 2A). See Video S1 for a video recording of a mosquito being hit, and Videos S2 and S3 for two video recordings of mosquitoes being missed by the swatter.

Using a statistical modeling approach, we investigated how the studied mosquito species adjust their flight dynamics to optimize their escape performance. We did this in four steps. First, we determined how the chance of being hit by the swatter (including virtual hits) differed between species, light conditions, and swatter mode (on/off). Second, we studied how baseline protean flight behavior affected the escape performance. Third, we determined how the swatter-induced escape maneuver dynamics affected escape performance. Finally, we quantified the relative contributions of baseline protean flight behavior and escape maneuver dynamics to the overall escape performance.

Modeling the probability of being hit by the mechanical swatter

Using a Bayesian generalized linear model (B-GLM), we first tested how the probability of being hit by the swatter (either real or virtual) varied between species, light conditions, and swatter activation (on/off) (Figures 2D–2I). Here, we modeled light as a binary variable, either the light condition during which each species naturally host-seeks (dark for *Anopheles* and overcast daylight for *Aedes*) or the other light conditions combined. From here on, we will refer to these as the reference light conditions and the altered light conditions, respectively. After doing a forward selection procedure (see STAR Methods), the minimal model contained four predictors: swatter activation (on/off), species, and reference light versus altered light (modeled as the interactions between *Anopheles* or *Aedes* with the light condition). An effect was found to be significant (i.e., null-hypothesis rejected) if the 89% highest density interval (HDI) of the standardized effect size (SES) was found completely outside of the region of practical equivalence (ROPE = [−0.1, 0.1]) (Figures 2G–2I).

The model shows that *Aedes* mosquitoes had a significantly lower probability of being hit than *Anopheles* mosquitoes (P_{hit} = 6% and P_{hit} = 13%, respectively; SES mode = −0.75). Also, *Anopheles* mosquitoes were significantly less likely to be hit by the swatter if they were flying in their reference dark conditions (SES mode = 0.42). A comparable trend in reference versus altered light was observed for *Aedes* mosquitoes, but it was not significant (Figure 2I). We finally compared the estimated means of hit probabilities between light conditions (Figures 2J and 2K). Results show that *Anopheles* has a lower chance of being hit in the reference dark condition, both with the swatter on and off (Figures 2J and 2K). For *Aedes* mosquitoes, hit percentages only differed significantly among light conditions when the swatter was activated, as it was increased in the intermediate sunrise condition (Figure 2K).

The baseline protean flight behavior of mosquitoes explains the low number of hits

We tested whether the previously found low numbers of (real and virtual) hits were the result of a baseline protean flight behavior of mosquitoes. The temporal dynamics of the distance between mosquito and swatter showed that the average mosquito was flying at a minimal distance of more than 6 cm from the swatter, even if the swatter was turned off (Figures 3A and 3C). This explains why most mosquitoes were not hit, which would have occurred when the distance between mosquito and swatter was reduced to zero. Video S2 shows an example of a flying mosquito missed by the swatter, apparently without having to perform an evasive maneuver.

To explain why most mosquitoes did not get closer to the swatter, we determined the temporal dynamics of the flight path deviation as the distance between the real flight path and the predicted one (d_{path}, Figure 3B). With the swatter turned off, the mean flight path deviation increased approximately linearly with time, directly after the moment of triggering (Figure 3D). At the moment of maximum virtual swatter extension (time t = 0 s), the flight path deviation was on average 8 cm.

collision probability for a given condition. Red crosses indicate data points used in the B-GLM. Highest density intervals (HDI) and probability density functions (PDF) are shown for all tested conditions.

(G–I) Distributions of the standardized slopes means β_1, β_2, and β_3. The null-hypothesis was rejected if the 89% highest density intervals (HDI) was outside the region of practical equivalence (ROPE). Here, all slopes differ significantly from zero except for the effect of *Aedes* in the reference or altered light conditions (yellow).

(J and K) Bayesian estimation of the mean collision probabilities in the various experimental conditions. Histograms of the associated standardized effect sizes (SES) are shown in Figure S2.

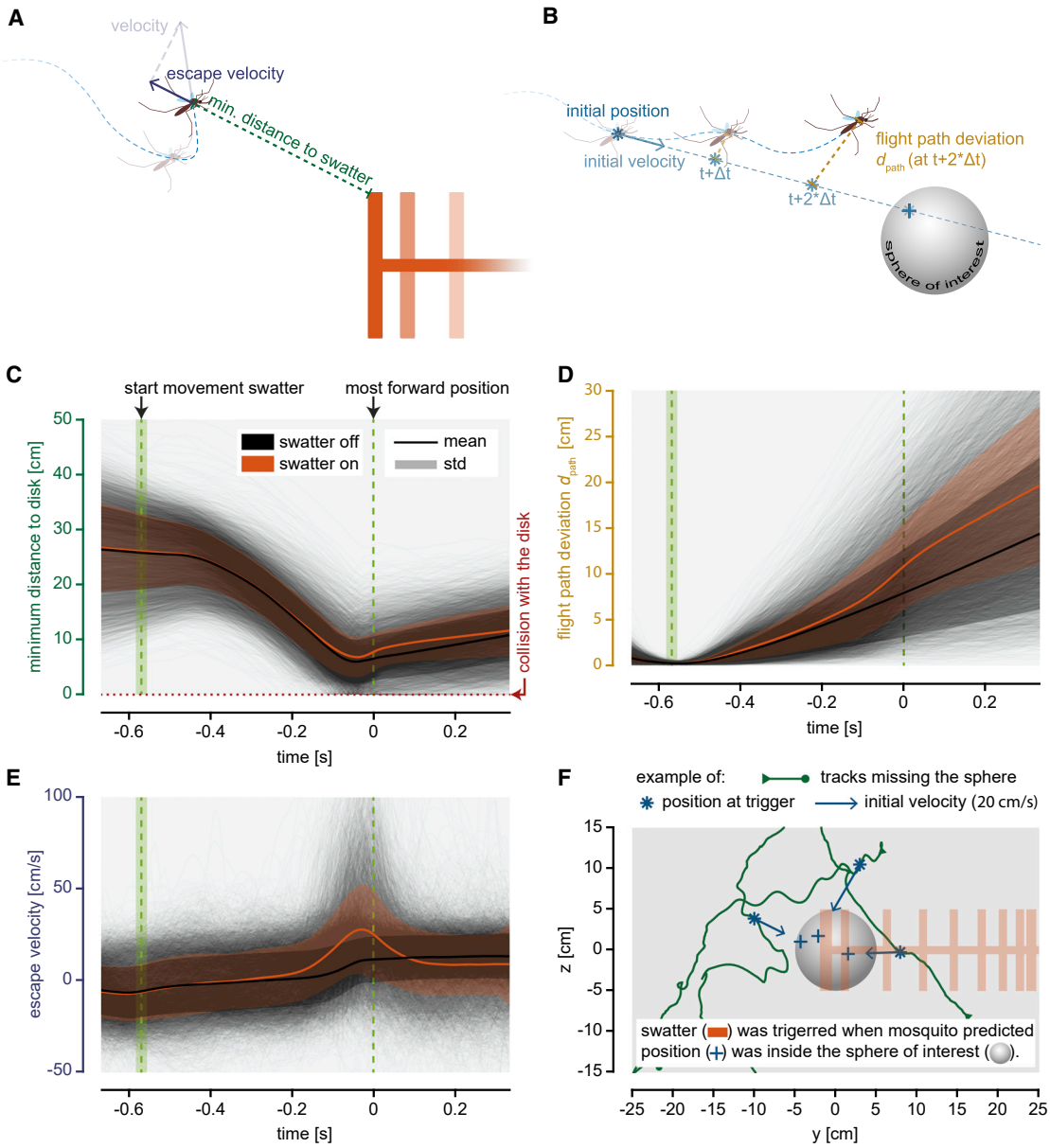

Figure 3. The majority of flying mosquitoes are missed by the swatter

(A and B) Definitions of the flight kinematics parameters: (A) escape velocity and the minimum distance between mosquito and swatter, and (B) the flight path deviation as the Euclidian distance of the mosquito from its predicted flight path.

(C–E) Temporal dynamics of the minimum distance between mosquito and swatter (real or virtual), distance from the predicted flight path, and escape velocity, respectively. Here, data for each recorded flight track are shown in gray; the mean and standard deviation of all tracks when the swatter was turned on and off are in orange and black, respectively.

(F) Flight tracks of mosquitoes that never entered the sphere in the middle of the arena, despite flying initially toward it and thereby triggering the swatter (blue data).

With the swatter turned on, the average flight path deviation of mosquitoes initially increased with time in a similar linear way as with the swatter turned off (control). However, just before the swatter reached the center of the arena and when it was closest to mosquitoes, this flight path deviation rapidly increased (Figure 3D). As a result, at t = 0 s the flight path deviation was on average 11 cm, 36% larger than for the control. This rapid increase in the flight path deviation elicited by the active swatter occurred when the escape flight velocity of the mosquitoes was maximal (Figure 3E).

Fast and curvy flight paths prior to swatter attack reduces the chance of being hit

To determine what flight kinematics characteristics are responsible for the baseline protean flight behavior, we characterized each flight prior to the swatter attack using the linear

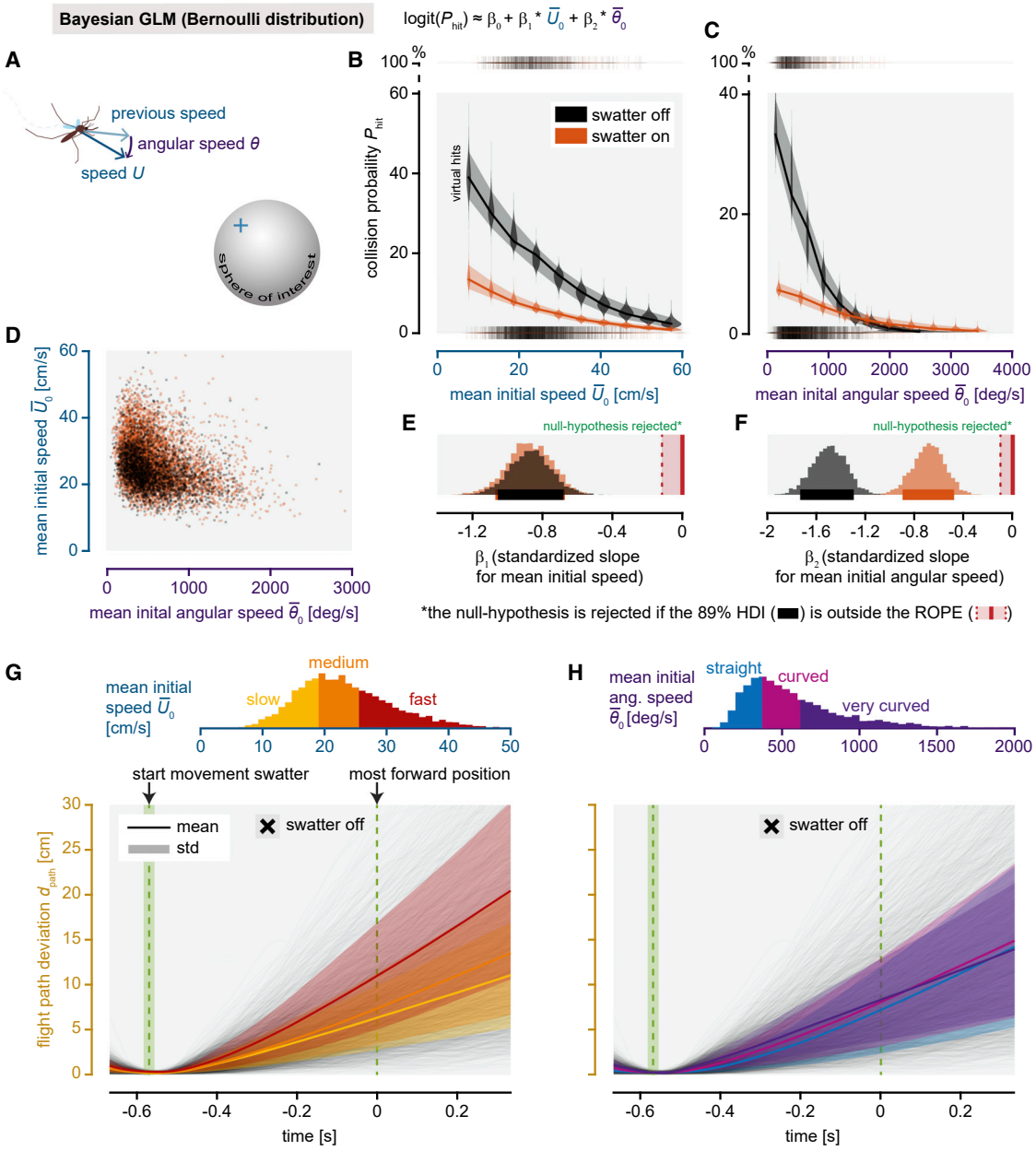

Figure 4. The initial flight conditions strongly affect collision probability

(A) Definition of the initial flight speed and angular speed of a mosquito, at the moment when the swatter was triggered.

(B and C) Results of the Bayesian-GLM that models the mean collision probability as a function of the initial linear and angular flight speeds and swatter mode (on or off, see legend in B). Each panel is a slice plot showing only the effect of one predictor, with the other predictors set at their mean values. Distributions are estimates of the mean collision probability for a given condition. Highest density intervals (HDI) are also showed.

(D) Mean initial linear and angular speeds of all recorded tracks, color-coded with the swatter mode.

(E and F) Distributions of the means of the standardized slopes β_1 and β_2 show that all effects are significant (i.e., the 89% highest density intervals (HDI) was outside the region of practical equivalence (ROPE)).

(G and H) Temporal dynamics of the distance to the predicted flight path, at (G) three initial speed bins (slow, medium, and fast), and (H) three initial angular speed bins (straight, low-curved, and high-curved flights). See histograms on the top for the binning definitions. Gray lines show results of the separate flight tracks and colored data show the mean and standard deviations for each binned subgroup.

and angular flight speeds at the moment of triggering (U_0 and θ_0, respectively; Figure 4A). We then used a B-GLM to determine how these flight characteristics affect the probability of being hit (real or virtual; Figures 4B, 4C, 4E, and 4F). The minimal model showed that the hit chance rapidly decreases with an increase in both the linear and angular speeds, and the effect is larger when the swatter is turned off (Figures 4B and 4C).

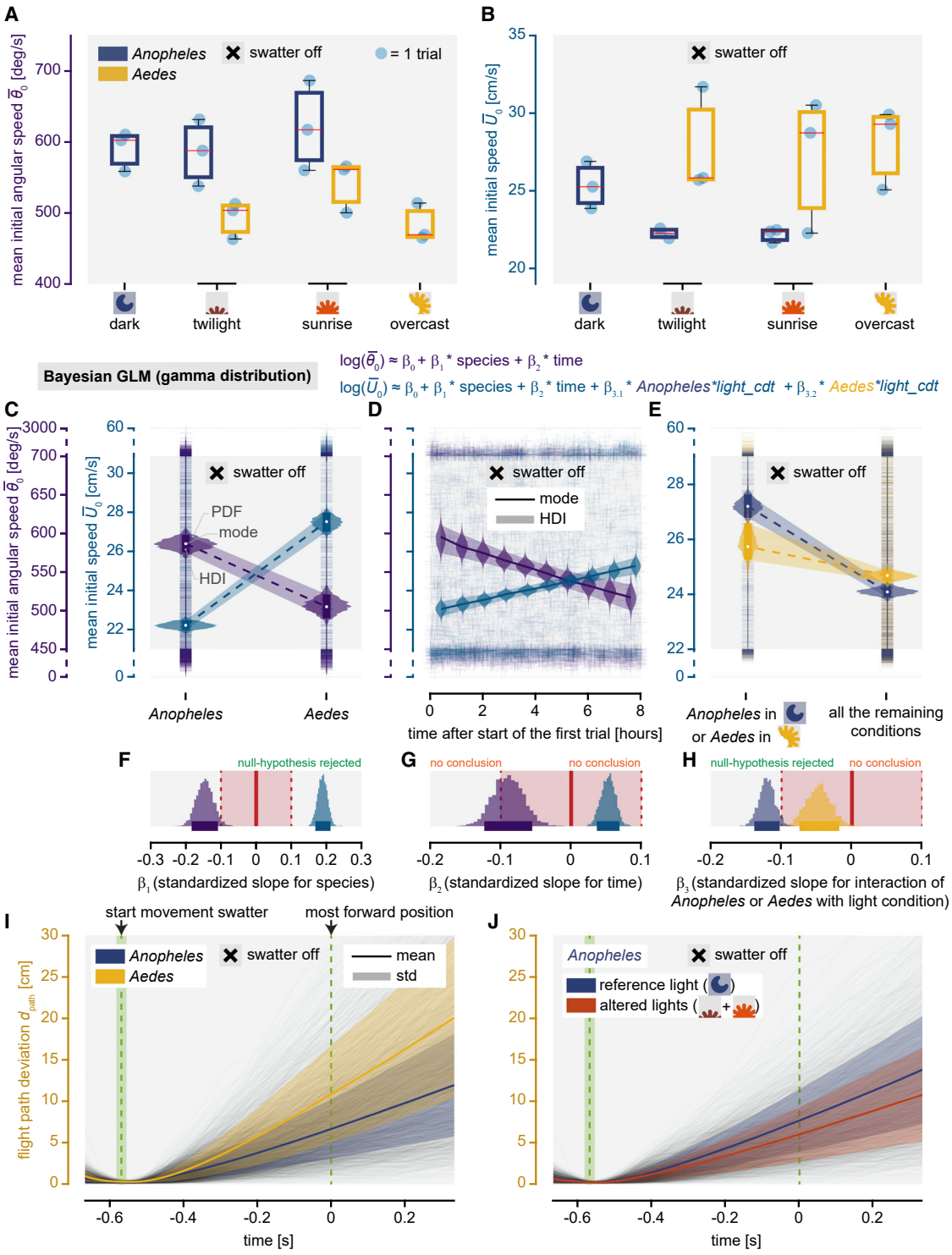

Figure 5. The initial flight speed varies with experimental conditions

(A and B) The mean initial linear and angular flight speed of mosquitoes in the various test conditions of the control experiment (swatter turned off). Boxplots of various flight kinematics metrics can be found in Figure S5.

(C–E) Results of the two Bayesian-GLMs that modeled the mean initial flight speed and mean angular speed as a function of (C) species, (D) time, and (E) light condition for the control experiments only (swatter off). Each panel is a slice plot showing only the effect of one predictor, with the others set at their mean values. Highest density intervals (HDI) and probability density functions (PDF) are shown for all tested conditions.

(F–H) Distributions of the means of the standardized slopes β_1, β_2, and β_3. Here, the null-hypothesis was rejected if the 89% highest density intervals (HDI) was outside the region of practical equivalence (ROPE).

(legend continued on next page)

To study the underlying cause of this, we tested how the temporal dynamics of the flight path deviation varied with initial linear and angular flight speed (Figures 4G and 4H, respectively). This shows that initially faster flying mosquitoes deviated more from their predicted flight paths (Figure 4G), but this flight path deviation did not clearly vary with their initial angular speed (Figure 4H).

Anopheles and Aedes mosquitoes use different mechanisms to maximize their baseline protean behavior

The distribution of linear and angular speeds (Figure 4D) suggests that there is a trade-off between high linear speeds and high angular speeds; thus, mosquitoes could only adjust their flight dynamics to maximize one of the two. Using B-GLMs, we modeled how the initial linear and angular flight speeds (Figures 5A and 5B) varied between species, with light conditions, and with time during the experimental trial (Figures 5C–5H). Because we were interested here in the baseline protean flight behavior, we performed this analysis on the control flights (swatter off) in order to exclude escape responses.

Comparing the flight characteristics between the species shows that *Anopheles* flies with a 16% higher angular speed and a 16% lower linear flight speed than *Aedes* (Figures 5C and 5F). The temporal dynamics of the flight path deviation shows that the faster flying *Aedes* mosquitoes deviate more from their predicted flight path than the slower flying *Anopheles* mosquitoes (Figures 5I, 6A, and 6B). As a result, at the moment of maximum virtual swatter extension (t = 0 s) *Aedes* has a 50% higher flight path deviation than *Anopheles* (d_{path} = 12 cm and d_{path} = 8 cm, respectively). We also tested how linear and angular flight speeds varied with time (Figure 5D), but the observed trends were not significant (Figure 5G).

Finally, we tested how linear and angular flight speeds varied with light conditions for the two species (Figures 5E and 5H). This showed that *Anopheles* mosquitoes flew faster in their reference light condition (dark) than in the altered conditions. For *Aedes* mosquitoes, we observed a similar trend of higher flight speeds in the reference light condition (overcast daylight), but the difference was not significant. Angular speed did not differ significantly between the reference and altered light conditions.

For *Anopheles*, flight path deviation increased with time more rapidly in the dark reference condition than in the altered light condition (Figures 5J). As a result, at t = 0 s, this deviation was on average 40% larger in the dark than for the other conditions combined (d_{path} = 7 cm and d_{path} = 4 cm, respectively). This indicates that, when flying in the dark, *Anopheles* mosquitoes maximized their baseline protean behavior by increasing their flight speed.

Both mosquito species exhibit fast swatter-induced evasive maneuvers more often in brighter light conditions

Following our analysis of the baseline protean flight behavior, we studied the evasive maneuver dynamics of the mosquitoes. For this, we combined a hidden Markov model (HMM) and a B-GLM to estimate the probability that the swatter triggered a rapid escape maneuver (P_{escape}) in the various experimental conditions and how this varied between species (Figures 6C and 6D). Videos S2 and S3 show examples of two non-hit mosquitoes, where one performed an escape maneuver and the other did not.

The combined HMM and B-GLM analysis showed that *Anopheles* mosquitoes that were attacked by the swatter had a 38% higher chance of performing a fast escape maneuver than *Aedes* (Figures 6E and 6H). Also, fast escape probability was positively correlated with the logarithm of light condition luminance, whereby P_{escape} increases with light intensity from 14% in the dark to 25% in overcast daylight (Figures 6F and 6I). Finally, when including the effect of luminance in the model, the fast escape probability did not differ significantly between the reference and altered light conditions, for both species (Figures 6G and 6J).

The escape strategies of day and night-active mosquitoes vary differently with light conditions

Thus, mosquitoes rely both on baseline protean flight behavior and escape maneuverability to avoid a rapidly looming object (Figures 5 and 6, respectively). In this analysis section, we tested how the relative contribution of both behaviors affects escape performance and how this differs between species and light conditions (Figure 7).

For this, we quantified the escape performance of the flying mosquito using its flight path deviation at time t = 0 s (d_0) when the swatter reached its most forward position (Figures 3B and 3D). Using a B-GLM, we found that this flight path deviation was on average 45% higher when the swatter was turned on (Figures 7A, 7D, and 7G), and it was 63% higher for *Aedes* than for *Anopheles* (Figures 7B, 7C, 7E, and 7H). Additionally, *Anopheles* mosquitoes deviated more from their predicted path when they flew in the dark reference condition than in the other light conditions (Figures 7B, 7C, 7F, and 7I). A similar trend was found for the reference overcast condition of *Aedes*, but this was not significant, owing to the small effect size (Figures 7F and 7I).

These results are very much in line with the results of the B-GLM used to model the probability of being hit by the swatter (Figures 2D–2I), suggesting that the deviation from predicted position is a good metric to describe escape performance. Therefore, we used this parameter to quantify the relative contributions of baseline protean flight behavior and escape maneuverability to the escape performance. For this, we defined the relative baseline protean contribution to flight path deviations as $R_{protean} = d_{off}/d_{on} \cdot 100\%$ (Figures 7J–7L), where d_{off} and d_{on} are the flight path deviations at t = 0 s when the swatter was turned off and on, respectively. Note that d_{off} is the result of only the baseline protean behavior, and d_{on} is the result of the baseline protean behavior and the escape maneuver combined. Thus, $R_{protean}$ = 100% if a flight path deviation is fully caused by the baseline protean behavior, and $R_{protean}$ = 0% when a flight path deviation is fully caused by the escape maneuver. The average *Anopheles* mosquito has a significantly higher mean relative baseline protean contribution in the dark ($R_{protean}$ = 90%) than in twilight ($R_{protean}$ =

(I and J) Temporal dynamics of the flight path deviation for all tracks when the swatter was turned off (control experiments). Gray lines show separate tracks, and the colored data show the mean and standard error for (I) *Anopheles* (blue) and *Aedes* (yellow), and (J) *Anopheles* in reference light (blue) and altered light (orange). Temporal dynamics of various flight kinematics parameters for the separate mosquito species and for the various track types can be found in Figures S6 and S7.

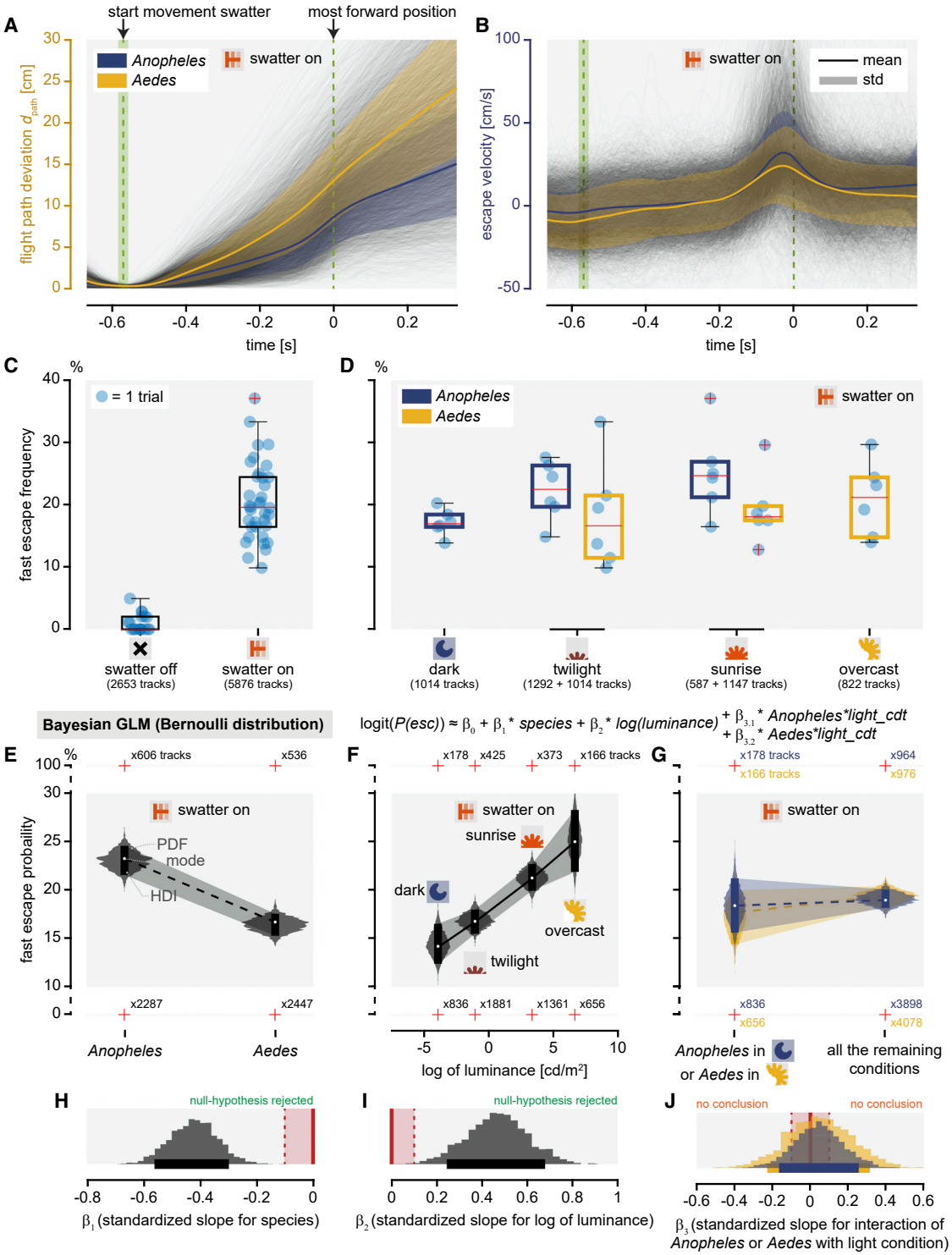

Figure 6. The probability of making a fast escape varies between species and with light condition

(A and B) Temporal dynamics of the flight path deviations and escape velocities of all flight tracks when the swatter was turned on. Gray lines show separate tracks, and the colored data show the mean and standard error for *Anopheles* (blue) and *Aedes* (yellow).

(C and D) Percentage of non-hit flight tracks that included a fast escape state, (C) for all flights with the swatter turned on or off, and (D) for the two separate species at various light conditions.

(legend continued on next page)

75%) or in sunrise ($R_{protean}$ = 79%). *Aedes* has the lowest relative protean contribution in the overcast daylight condition ($R_{protean}$ = 78%) and the highest $R_{protean}$ in sunrise ($R_{protean}$ = 89%).

DISCUSSION

We studied the escape performance of flying mosquitoes by testing how freely flying mosquitoes avoid being hit by an automated mechanical swatter, generating both visual cues and air movements. We tested how the attacked mosquitoes rely on their baseline flight path unpredictability and escape maneuverability to maximize escape performance. Finally, we studied how this differed between day-active and night-active mosquitoes and how escape dynamics varied with light intensities ranging from dark to overcast daylight.

Simulating a realistic attack

Of all 10,064 swatter attacks, only 8% lead to a collision between mosquito and swatter, highlighting the surprisingly high escaping performance of these flying mosquitoes. In our experiments, we triggered the mechanical swatter based on the prediction that a mosquito would fly into a sphere in the middle of the arena when and where the swatter would hit the mosquito (Figure 1D). Thus, at the time of triggering, the swatter was on an intercepting course with the flying mosquito. In addition, the swatter kinematics consists of a rapid linear attack movement that stops slightly past the predicted point of interception. Both the simplified prediction method and the single degree-of-freedom kinematics of our swatter might explain the low collision percentage.

The prediction method that we used to activate our swatter is similar to how humans and dragonflies have been found to attack moving targets,[11,35–38] although they both use more sophisticated prediction models than we used here. Unlike our swatter, humans and dragonflies are continuously updating their predictions, at least in bright light conditions.[39,40] However, updating a prediction is not always possible (e.g., when the target is occluded) and is limited by sensory and neuromuscular delays.[38]

The single degree-of-freedom kinematics of our mechanical swatter is analogous to the kinematics of a swatting hand but differs highly from the sophisticated attacks of flying predators.[10,11] Flying predators such as birds or dragonflies may pursue mosquitoes when hunting them, which would most likely increase capture success. Also, a swatting hand tends to continue its movement for longer than our swatter, which would also increase its swatting success.

This suggests that the simplified kinematics of our mechanical swatter is most likely the main cause of the low collision percentage. Nevertheless, the employed standardized simplified swatting kinematics allowed us to assess the effects of different treatments more precisely on the escape performance from a mechanical looming object. Also, the use of our mechanical swatter instead of the simpler visual looming targets used in previous studies,[18,41] allowed for the generation of a more realistic range of cues. Finally, the main conclusions of our study do not depend on the absolute number of collisions; thus, we expect similar effects of light conditions on the escape performance of mosquitoes in response to more sophisticated attacks.

Mosquitoes increase their escape performance using erratic flight behavior

Similar to the relatively low hit percentages of the active swatter, also during the control trials when the swatter was turned off, only 13% of the reconstructed mosquito flight tracks were virtually hit by the simulated in-silico swatter (Figure 2D). In other words, 13% of the mosquitoes would have been hit by the mechanical swatter if it had been turned on but would not have had any effect on the flight path of the mosquitoes. This low virtual hit percentage can be explained by the combination of the relatively high movement latency of the swatter (525 ms), its simple kinematics, and the unpredictable nature of the flight trajectories of the mosquitoes. Our analysis of the control experiments showed that, after triggering the virtual swatter, many mosquitoes deviated quickly from their predicted flight paths, which often resulted in avoiding a virtual hit without having to perform an evasive maneuver (Figure 3D). This flight behavior is interpreted as a kind of protean insurance against attacks that the mosquito could find difficult to detect or avoid.[15] Because the predators and hosts of mosquitoes have been found to wait for optimal conditions before eliciting an attack,[38,42] such erratic flight behavior should also reduce the chance of attack initialization.

Additionally, mosquitoes that flew faster and with a higher angular speed prior to the attack had a lower chance of being hit (Figures 4B and 4C) and deviated more from their initial flight path (Figures 4G and 4H). This indicates that flight unpredictability is modulated by the mosquitoes using their linear and angular flight speeds. By definition, these two variables cannot be considered as protean *sensu stricto*, as they do not describe behavior randomness; instead, linear and angular flight speeds most likely function as an amplification factor that increases the effect of an underlying unpredictability in the flight behavior (Figures 4G and 4H). These results are in line with previous findings showing that the targeting accuracy of humans is best predicted by an interaction between the speed and turn angle of the target.[17] Thus, by flying faster or with sharper turns, mosquitoes decrease the chance of being hit or caught by an attacker.

Finally, despite recent examples of learning and habituation among mosquitoes,[43,44] our results were inconclusive about the effect of time after the start of the experiments on mosquito escape behaviors (as shown in Figure 5D and by the fact that time-related predictors were otherwise left out of our minimal models).

Rapid escape maneuvers are induced by both airflow and visual cues produced by the looming object

Comparing the real and virtual hit percentages between the control and active swatter experiments (Figure 2A) shows that

(E–G) Results of the two Bayesian-GLMs that modeled the mean fast escape probability (with swatter on) as a function of (E) species, (F) light intensity, and (G) (non)reference light condition. Each panel is a slice plot showing only the effect of one predictor with the others set at their mean values. Highest density intervals (HDI) and probability density functions (PDF) are shown for all tested conditions.
(H–J) The distributions of the means of the standardized slopes show that β_1 and β_2 are significantly different from zero (i.e., the 89% highest density intervals (HDI) was outside the region of practical equivalence (ROPE)).

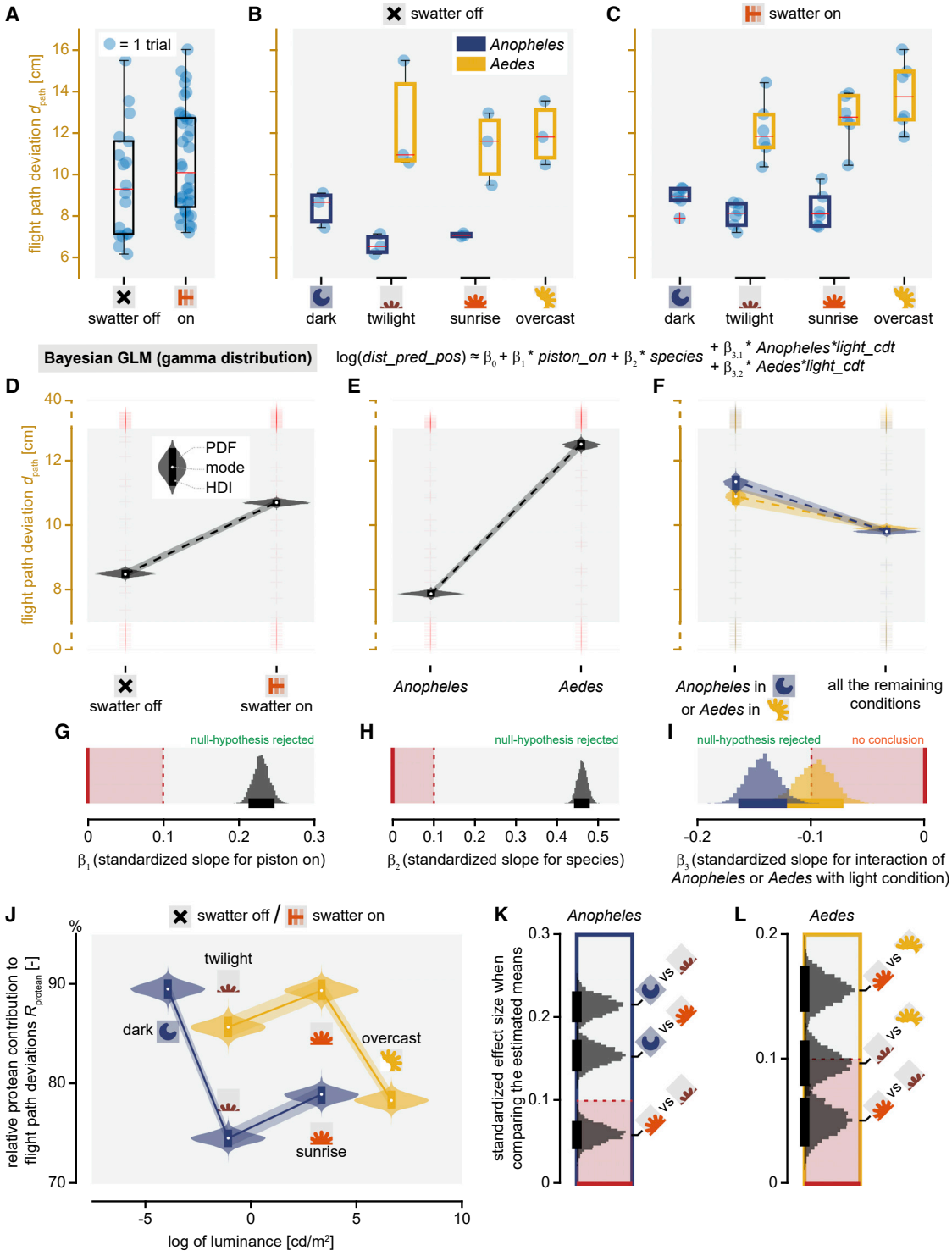

Figure 7. Flight path deviations differ between species and with experimental conditions

(A–C) The flight path deviation at the end of the (real or virtual) swatter attack for all non-hit tracks, with the swatter turned on and off (A) and for the two separate species at the various light conditions with the swatter turned off (B) and on (C).

(D–F) Results of the two Bayesian-GLMs that modeled the mean final path deviation of a flight that was not hit (by real or virtual swatter) as a function of (D) swatter mode (on or off), (E) species, and (F) (non)reference light condition. Each panel is a slice plot showing only the effect of one predictor with the others set at their mean values. Highest density intervals (HDI) and probability density functions (PDF) are shown for all tested conditions.

(G–I) Distributions of the means of the standardized slopes β_1, β_2, and β_3. Here, the null-hypothesis was rejected if the 89% highest density intervals (HDI) was outside the region of practical equivalence (ROPE).

(legend continued on next page)

evasive maneuvers reduce the chance of being hit by a factor of two (P_{hit} = 15% and P_{hit} = 8% of the virtual and real swatter, respectively). This suggests that the fast escape maneuvers that we identified in 19% of all flight tracks with the swatter activated were executed effectively because they halved the number of hits in the approximate 15% of mosquitoes at risk of being hit.

The temporal dynamics of the escape velocity of mosquitoes attacked by the swatter (Figures 3E and 6B) shows that the fast escapes mostly occurred just before the swatter entered the sphere of interest, where the mosquito was predicted to be hit. Our B-GLM analysis of the escape maneuvers shows that the probability of eliciting a fast escape is strongly affected by light intensity (Figures 6F and 6I), as it almost doubles from dark conditions to overcast daylight (P_{escape} = 14% and P_{escape} = 25% in the dark and overcast, respectively). Thus, visual detection of the swatter is an important factor in triggering an escape maneuver, showing that rapid escapes are, at least in large part, performed actively in bright light conditions. Because rapid escapes still occur in 14% of flights in full darkness, at least *Anopheles* mosquitoes also rely on the swatter-induced airflow to avoid being swatted. More research is needed to determine whether the swatter-induced airflow triggered an active escape maneuver, or if the airflow primarily causes a passive displacement of the mosquito.

Day-active *Aedes* mosquitoes exhibit higher escape performance than night-active *Anopheles*

Our analysis showed that both tested mosquito species, the night-active *Anopheles coluzzii* and the day-active *Aedes aegypti*, rely on baseline protean flight behavior and escape maneuverability to avoid being swatted. But they do this in strikingly different ways. The chance of being hit (real or virtual) by the swatter was twice as high for *Anopheles* mosquitoes than for *Aedes*, irrespectively of the light conditions or whether the swatter was turned on or off (Figure 2D). This was explained by the higher flight unpredictability of *Aedes*, quantified by their higher flight path deviation (Figure 5I). *Aedes* mosquitoes achieve this higher unpredictability by flying faster than *Anopheles* prior to the attack (Figure 5C). Interestingly, *Anopheles* mosquitoes fly slower but with higher angular speeds than *Aedes*, suggesting that they increase their baseline protean behavior using a different mechanism by flying at more curved flight paths (Figure 5C).

In contrast with the higher baseline protean performance of *Aedes* mosquitoes, *Anopheles* mosquitoes performed a higher number of rapid escape maneuvers than *Aedes* mosquitoes (Figure 6E). *Anopheles* mosquitoes are night-active and thus need to navigate complex environments with limited to no visual feedback. To be able to do this, they might be forced to fly consistently at relatively low flight speeds, and as a result, their protean performance is reduced compared with the faster flying *Aedes* mosquitoes. Our results suggest that *Anopheles* mosquitoes partially compensate for their reduced protean performance by flying at higher angular speeds and by responding more strongly to the looming object.

Night-active *Anopheles* mosquitoes have the highest escape performance in the dark

A striking result of our study is that *Anopheles* mosquitoes were least likely to be hit when flying in the lowest light condition (dark: luminance = 0.0201 cd/m^2) despite the greatly reduced visual cues compared with the other tested light conditions (Figure 2F). This suggests that these night-active mosquitoes adjust their flight behavior in such a way that they maximize their escape performance in the light conditions in which they are most at risk of being attacked.

In the dark, the collision probability of *Anopheles* with the swatter (virtual or physical) is similar between the experiments with the swatter off and on (Figures 2J and 2K, P_{hit} = 13% and P_{hit} = 7%, respectively). This suggests that *Anopheles* primarily increases its escape performance in the dark by increasing its baseline protean flight behavior, which is captured by the swatter off experiments. This is confirmed by the distinctly high relative contribution of baseline protean behavior on the flight path deviation in the dark (Figure 7J). This rapidly increases from 75% in twilight to 90% in darkness, highlighting the strong dependence of *Anopheles* on baseline protean behavior to avoid being swatted in the dark (Figure 7J).

We also determined the mechanisms that cause this high dependence on protean behavior, which is 2-fold. First, *Anopheles* perform the lowest number of fast escape maneuvers in the dark (Figure 6D), most likely due to the lack of visual looming cues. But this effect is relatively small between dark and twilight conditions (Figure 6F). In contrast, the enhanced baseline protean flight behavior of *Anopheles* in the dark is explained by the distinctly high flight speeds in this condition (Figures 5B and 5E). By flying relatively fast in the dark, *Anopheles* amplify the effect of their erratic curved flight behavior and therefore enhance their flight unpredictability in this condition. Thus, *Anopheles* exhibit enhanced baseline protean flight behavior in darkness and thereby increase their escape performance in dark conditions in which they are naturally active and host-seeking. Maintaining high flight unpredictability is most likely energetically costly. Therefore, *Anopheles* mosquitoes may only rely on such an increased level of protean insurance in the light conditions where they are at high risk of being swatted.

Day-active *Aedes* mosquitoes show enhanced escape performance in overcast daylight

In contrast with *Anopheles*, the day-active *Aedes* mosquitoes exhibit the lowest collision probabilities in the brightest tested light conditions (Figure 2C). Although the collision probability in overcast daylight was not significantly different from the other light conditions combined (Figures 2F and 2I), it was significantly lower than in sunrise conditions with the swatter turned on (Figure 2K). This suggests that the day-active *Aedes* mosquitoes also adjust their flight behavior in function of the light conditions,

(J) Bayesian estimation of the means of the relative baseline protean contribution to flight path deviations ($R_{protean}$) for non-hit *Anopheles* (blue) and *Aedes* (yellow) in the various light conditions.
(K and L) Standardized effect size of the comparisons of the estimated $R_{protean}$ means between light conditions, for non-hit *Anopheles* (K) and *Aedes* (L). Black HDI distributions outside the red ROPE box depict significant differences.

allowing them to maximize their escape performance in the conditions in which they are most at risk of being attacked. Our analysis of the baseline protean flight behavior and escape maneuver dynamics allowed us to identify how *Aedes* maximized their escape performance in the high light conditions. The escape performance of *Aedes* in the control experiments with the swatter turned off did not change with light intensity (Figure 2J, respectively), showing that *Aedes* mosquitoes did not modulate their baseline protean behavior with light. This was confirmed by the equally non-significant change in linear and angular flight speeds of *Aedes* under varying light conditions (Figure 5). In contrast, fast escape probability increased rapidly with light intensity (Figure 6F), suggesting that instead of modulating their baseline protean behavior, *Aedes* primarily increased their escape performance with light intensity by enhancing their escape maneuverability.

Our analysis of the relative contributions of baseline protean flight behavior and escape maneuverability on escape performance confirmed this (Figure 7). In the highest overcast light condition in which *Aedes* exhibited enhanced escape performance, the relative contribution of baseline protean behavior was particularly low (Figure 7J). This highlights that here *Aedes* rely to a relatively large extent on escape maneuverability to avoid being swatted. Our results confirmed that *Aedes* mosquitoes exhibit increased escape performance in overcast daylight, which they achieve primarily by enhancing their escape maneuverability. These rapid escapes in bright light are most likely triggered by visual detection of the looming object.

Escape flight behavior and evolutionary adaptations in diurnal and nocturnal mosquitoes

In this study, we combined sophisticated biomechanics experiments with a detailed two-species comparative analysis approach to identify the differences in escape flight behavior between a diurnal and nocturnal mosquito species. Such two-species comparative analysis cannot be used to directly prove evolutionary adaptations because this would require comparative analyses of a larger number of mosquito species.[45–47] We limited ourselves to this two-species comparative approach because of the time-consuming and complex nature of our biomechanics study. A future comparative study on multiple species could explicitly address the underlying evolutionary adaptations of diurnal and nocturnal flying insects. To do so, one should use a simpler approach to measure escape performance metrics, such as escape speed and free-flight protean behavior, and control for variations in morphological traits (such as wing loading and wing shape) and ecology (such as habitat and host preference).[45,46]

CONCLUSIONS

Flying mosquitoes attacked by a looming object possess a good escape performance due to both their hard-to-predict flight paths and their effective escape maneuvers. Flight path baseline unpredictability is modulated by both the linear and angular speeds of the undisturbed flying mosquito; escape maneuvers are triggered by both visual cues and the airflow induced by the attacker. The night-active *Anopheles* mosquitoes exhibited maximum escape performance in the dark, whereas day-active *Aedes* showed enhanced escape performance in the highest daylight light intensity. Thus, for both species, escape performance is enhanced in the light conditions in which they naturally seek blood hosts and are thus most at risk of being swatted by defensive hosts. Finally, for both species, the baseline unpredictability of their flight paths had the largest effect on escape performance. This protean insurance against attacks might be more important for flying insects than is often assumed.

STAR★METHODS

Detailed methods are provided in the online version of this paper and include the following:

- KEY RESOURCES TABLE
- RESOURCE AVAILABILITY
  - Lead contact
  - Materials availability
  - Data and code availability
- EXPERIMENTAL MODEL AND SUBJECT DETAILS
  - Experimental animals
- METHOD DETAILS
  - The flight arena
  - Experimental procedure
- QUANTIFICATION AND STATISTICAL ANALYSIS
  - Analysis of three-dimensional flight tracks
  - Bayesian generalized linear model development
  - Hidden Markov model development
  - Analysing the escape performance of mosquitoes

SUPPLEMENTAL INFORMATION

Supplemental information can be found online at https://doi.org/10.1016/j.cub.2022.01.036.

ACKNOWLEDGMENT

We thank Jasper Eikelboom and Henjo de Knegt for introducing us to Hidden Markov Models and the rest of the animal movement discussion group for the many exciting meetings. We thank Andres Hagmayer for his precious advice on using Bayesian-GLMs. We thank Tessa Visser, Pieter Rouweler, Kimmy Reijngoudt, André Gidding, and Frans van Aggelen for rearing the mosquitoes in Wageningen.

This work was supported by a doctoral fellowship from the Wageningen Institute of Animal Sciences (WIAS) to A.C.. F.T.M. was supported by a grant from the Netherlands Organization for Scientific Research (NWO/VI.Vidi.193.054).

AUTHOR CONTRIBUTIONS

A.C. and F.T.M. conceived and designed the experiments. A.C. and R.P.M.P. designed and built the experimental setup. A.S. developed the real-time tracking software flydra and provided support for integrating it in the experimental setup. A.C. designed and build the automatic experimental system. A.C. performed the experiments. A.C. analyzed the data. F.T.M., J.S., and J.L.v.L. provided support for the analysis. A.C. wrote the first draft of the manuscript. All authors commented the manuscript. All authors read and approved the final manuscript.

DECLARATION OF INTERESTS

The authors declare no competing interests.

Received: October 5, 2021
Revised: December 21, 2021
Accepted: January 12, 2022
Published: February 7, 2022

REFERENCES

1. Walker, E.D., and Edman, J.D. (1985). The influence of host defensive behavior on mosquito (Diptera: culicidae) biting persistence. J. Med. Entomol. *22*, 370–372.
2. Darbro, J.M., and Harrington, L.C. (2007). Avian defensive behavior and blood-feeding success of the West Nile vector mosquito, Culex pipiens. Behav. Ecol. *18*, 750–757.
3. Edman, J.D., and Scott, T.W. (1987). Host defensive behaviour and the feeding success of mosquitoes. Int. J. Trop. Insect Sci. *8*, 617–622.
4. Reid, J.N., Hoffmeister, T.S., Hoi, A.G., and Roitberg, B.D. (2014). Bite or flight: the response of mosquitoes to disturbance while feeding on a defensive host. Entomol. Exp. Appl. *153*, 240–245.
5. Matherne, M.E., Cockerill, K., Zhou, Y., Bellamkonda, M., and Hu, D.L. (2018). Mammals repel mosquitoes with their tails. J. Exp. Biol. *221*, jeb178905.
6. Edman, J.D., Day, J.F., and Walker, E.D. (1984). Field confirmation of laboratory observations on the differential antimosquito behavior of herons. Condor *86*, 91.
7. Medlock, J.M., and Snow, K.R. (2008). Natural predators and parasites of British mosquitoes – a review. Eur. Mosq. Bull. *25*, 1–11.
8. Yuval, B., and Bouskila, A. (1993). Temporal dynamics of mating and predation in mosquito swarms. Oecologia *95*, 65–69.
9. Roitberg, B.D., Mondor, E.B., and Tyerman, J.G.A. (2003). Pouncing spider, flying mosquito: blood acquisition increases predation risk in mosquitoes. Behav. Ecol. *14*, 736–740.
10. Pal, S. (2015). Dynamics of aerial target pursuit. Eur. Phys. J. Spec. Top. *224*, 3295–3309.
11. Mischiati, M., Lin, H.T., Herold, P., Imler, E., Olberg, R., and Leonardo, A. (2015). Internal models direct dragonfly interception steering. Nature *517*, 333–338.
12. Olberg, R.M., Seaman, R.C., Coats, M.I., and Henry, A.F. (2007). Eye movements and target fixation during dragonfly prey-interception flights. J. Comp. Physiol. A Neuroethol. Sens. Neural Behav. Physiol. *193*, 685–693.
13. Mizutani, A., Chahl, J.S., and Srinivasan, M.V. (2003). Motion camouflage in dragonflies. Nature *423*, 604.
14. Ghose, K., Horiuchi, T.K., Krishnaprasad, P.S., and Moss, C.F. (2006). Echolocating bats use a nearly time-optimal strategy to intercept prey. PLoS Biol *4*, e108.
15. Humphries, D.A., and Driver, P.M. (1970). Protean defence by prey animals. Oecologia *5*, 285–302.
16. Moore, T.Y., Cooper, K.L., Biewener, A.A., and Vasudevan, R. (2017). Unpredictability of escape trajectory explains predator evasion ability and microhabitat preference of desert rodents. Nat. Commun. *8*, 440.
17. Richardson, G., Dickinson, P., Burman, O.H.P.P., Pike, T.W., Richardson, G., Dickinson, P., and Burman, O.H.P.P. (2018). Unpredictable movement as an anti-predator strategy. Proc. R. Soc. Lond. B *285*, 20181112.
18. Muijres, F.T., Elzinga, M.J., Melis, J.M., and Dickinson, M.H. (2014). Flies evade looming targets by executing rapid visually directed banked turns. Science *344*, 172–177.
19. Santer, R.D., Rind, F.C., and Simmons, P.J. (2012). Predator versus prey: locust looming-detector neuron and behavioural responses to stimuli representing attacking bird predators. PLoS One *7*, e50146.
20. Cheng, B., Tobalske, B.W., Powers, D.R., Hedrick, T.L., Wethington, S.M., Chiu, G.T.C., and Deng, X. (2016). Flight mechanics and control of escape manoeuvres in hummingbirds. I. Flight kinematics. J. Exp. Biol. *219*, 3518–3531.
21. Corcoran, A.J., and Conner, W.E. (2016). How moths escape bats: predicting outcomes of predator-prey interactions. J. Exp. Biol. *219*, 2704–2715.
22. Cribellier, A., Van Erp, J.A., Hiscox, A., Lankheet, M.J., Van Leeuwen, J.L., Spitzen, J., Muijres, F.T., and Erp, J.A. Van. (2018). Flight behaviour of malaria mosquitoes around odour-baited traps: capture and escape dynamics. R. Soc. Open Sci. *5*, 180246.
23. Hawkes, F., and Gibson, G. (2016). Seeing is believing: the nocturnal malarial mosquito *Anopheles coluzzii* responds to visual host-cues when odour indicates a host is nearby. Parasit. Vectors *9*, 320.
24. Thorsteinson, A.J., Bracken, G.K., and Hanec, W. (1965). The orientation of horse flies and deer flies (Tabanidae, Diptera): III. The use of traps in the study of orientation of Tabanids in the field. Entomolia Exp. Appl. *8*, 189–192.
25. Townes, H. (1962). Design for a malaise trap. Proc. Entomol. Soc. Washingt. *64*, 253–262.
26. McMeniman, C.J.J., Corfas, R.A.A., Matthews, B.J.J., Ritchie, S.A.A., and Vosshall, L.B.B. (2014). Multimodal integration of carbon dioxide and other sensory cues drives mosquito attraction to humans. Cell *156*, 1060–1071.
27. Van Breugel, F., Riffell, J.a., Fairhall, A., and Dickinson, M.H. (2015). Mosquitoes use vision to associate odor plumes with thermal targets. Curr. Biol. *25*, 2123–2129.
28. Cardé, R.T. (2015). Multi-cue integration: how female mosquitoes locate a human host. Curr. Biol. *25*, R793–R795.
29. Fuller, S.B., Straw, A.D., Peek, M.Y., Murray, R.M., and Dickinson, M.H. (2014). Flying Drosophila stabilize their vision-based velocity controller by sensing wind with their antennae. Proc. Natl. Acad. Sci. USA *111*, E1182–E1191.
30. Chapman, T., and Webb, B. (1999). A neuromorphic hair sensor model of wind-mediated escape in the cricket. Int. J. Neural Syst. *9*, 397–403.
31. Triblehorn, J.D., and Yager, D.D. (2006). Wind generated by an attacking bat: anemometric measurements and detection by the praying mantis cercal system. J. Exp. Biol. *209*, 1430–1440.
32. Dupuy, F., Steinmann, T., Pierre, D., Christidés, J.P., Cummins, G., Lazzari, C., Miller, J., and Casas, J. (2012). Responses of cricket cercal interneurons to realistic naturalistic stimuli in the field. J. Exp. Biol. *215*, 2382–2389.
33. Combes, S.A., Rundle, D.E., Iwasaki, J.M., and Crall, J.D. (2012). Linking biomechanics and ecology through predator-prey interactions: flight performance of dragonflies and their prey. J. Exp. Biol. *215*, 903–913.
34. Takken, W., and Verhulst, N.O. (2013). Host preferences of blood-feeding mosquitoes. Annu. Rev. Entomol. *58*, 433–453.
35. Nakata, T., Henningsson, P., Lin, H.T., and Bomphrey, R.J. (2020). Recent progress on the flight of dragonflies and damselflies. Int. J. Odonatol. *23*, 41–49.
36. Wiederman, S.D., Fabian, J.M., Dunbier, J.R., and O'Carroll, D.C. (2017). A predictive focus of gain modulation encodes target trajectories in insect vision. Elife *6*, e26478.
37. Soechting, J.F., and Flanders, M. (2008). Extrapolation of visual motion for manual interception. J. Neurophysiol. *99*, 2956–2967.
38. Mrotek, L.A., and Soechting, J.F. (2007). Target interception: hand-eye coordination and strategies. J. Neurosci. *27*, 7297–7309.
39. Brenner, E., and Smeets, J.B.J. (2018). Continuously updating one's predictions underlies successful interception. J. Neurophysiol. *120*, 3257–3274.
40. Zhao, H., and Warren, W.H. (2015). On-line and model-based approaches to the visual control of action. Vision Res *110*, 190–202.
41. Card, G.M. (2012). Escape behaviors in insects. Curr. Opin. Neurobiol. *22*, 180–186.
42. Lin, H.T., and Leonardo, A. (2017). Heuristic rules underlying dragonfly prey selection and interception. Curr. Biol. *27*, 1124–1137.
43. Vinauger, C., Lahondère, C., Wolff, G.H., Locke, L.T., Liaw, J.E., Parrish, J.Z., Akbari, O.S., Dickinson, M.H., and Riffell, J.A. (2018). Modulation of host learning in *Aedes aegypti* mosquitoes. Curr. Biol. *28*, 333–344.e8.
44. Baglan, H., Lazzari, C., and Guerrieri, F. (2017). Learning in mosquito larvae (*Aedes aegypti*): habituation to a visual danger signal. J. Insect Physiol. *98*, 160–166.

45. Berberi, I., Segre, P.S., Altshuler, D.L., and Dakin, R. (2020). Unpredictable hummingbirds: flight path entropy is constrained by speed and wing loading. bioRxiv. https://doi.org/10.1101/2020.08.11.246926.
46. Le Roy, C., Amadori, D., Charberet, S., Windt, J., Muijres, F.T., Llaurens, V., and Debat, V. (2021). Adaptive evolution of flight in Morpho butterflies. Science *374*, 1158–1162.
47. Garland, T., and Adolph, S.C. (1994). Why not to do two-species comparative studies: limitations on inferring adaptation. Physiol. Zool. *67*, 797–828.
48. Steyvers, M., and Kalish, M. (2014). MATJAGS, a Matlab interface for JAGS.
49. Kruschke, J.K. (2013). Bayesian estimation supersedes the t test. J. Exp. Psychol. Gen. *142*, 573–603.
50. Winter, N. (2016). GitHub – NilsWinter/matlab-bayesian-estimation: Matlab toolbox for bayesian estimation.
51. Murphy, K. (1998). Hidden Markov Model (HMM) toolbox for Matlab.
52. Gibson, G. (1995). A behavioural test of the sensitivity of a nocturnal mosquito, Anopheles gambiae, to dim white, red and infra-red light. Physiol. Entomol. *20*, 224–228.
53. Stowers, J.R., Hofbauer, M., Bastien, R., Griessner, J., Higgins, P., Farooqui, S., Fischer, R.M., Nowikovsky, K., Haubensak, W., Couzin, I.D., et al. (2017). Virtual reality for freely moving animals. Nat. Methods *14*, 995–1002.
54. Straw, A.D., Branson, K., Neumann, T.R., and Dickinson, M.H. (2011). Multi-camera real-time three-dimensional tracking of multiple flying animals. J. R. Soc. Interface *8*, 395–409.
55. Open, C.V. (2014). OpenCV documentation: camera calibration and 3D reconstruction.
56. Dekker, T., and Cardé, R.T. (2011). Moment-to-moment flight manoeuvres of the female yellow fever mosquito (*Aedes aegypti* L.) in response to plumes of carbon dioxide and human skin odour. J. Exp. Biol. *214*, 3480–3494.
57. Cooperband, M.F., and Cardé, R.T. (2006). Orientation of Culex mosquitoes to carbon dioxide-baited traps: flight manoeuvres and trapping efficiency. Med. Vet. Entomol. *20*, 11–26.
58. Spitzen, J., Spoor, C.W., Grieco, F., ter Braak, C., Beeuwkes, J., van Brugge, S.P., Kranenbarg, S., Noldus, L.P.J.J., van Leeuwen, J.L., and Takken, W. (2013). A 3D analysis of flight behavior of *Anopheles gambiae sensu stricto* malaria mosquitoes in response to human odor and heat. PLoS One *8*, e62995.
59. Kruschke, J.K. (2010). Bayesian data analysis. Wiley Interdiscip. Rev. Cogn. Sci. *1*, 658–676.
60. Dienes, Z. (2011). Bayesian versus orthodox statistics: which side are you on? Perspect. Psychol. Sci. *6*, 274–290.
61. Plummer, M. (2003). JAGS: A program for analysis of Bayesian graphical models using Gibbs sampling. In Proceedings of the 3rd International Conference on Distributed Statistical Computing, pp. 1–10.
62. Kruschke, J.K., and Liddell, T.M. (2018). The Bayesian new statistics: hypothesis testing, estimation, meta-analysis, and power analysis from a Bayesian perspective. Psychon. Bull. Rev. *25*, 178–206.
63. Zuur, A.F., Hilbe, J.M., and Ieno, E.N. (2013). A Beginner's Guide to GLM and GLMM with R (Highland Statistics).
64. Gelman, A. (2008). Scaling regression inputs by dividing by two standard deviations. Stat. Med. *27*, 2865–2873.
65. Schielzeth, H. (2010). Simple means to improve the interpretability of regression coefficients. Methods Ecol. Evol. *1*, 103–113.
66. Gelman, A., and Rubin, D.B. (1992). Inference from iterative simulation using multiple sequences. Statist. Sci. *7*, 457–472. https://doi.org/10.1214/ss/1177011136.

STAR★METHODS

KEY RESOURCES TABLE

REAGENT or RESOURCE	SOURCE	IDENTIFIER
Deposited data		
Database S1	DRYAD repository as part of this paper	https://doi.org/10.5061/dryad.ttdz08m09
Experimental models: Organisms/strains		
Anopheles coluzzii	Via Prof. M. Coluzzi, Suakoko, Liberia, 1987	Suakoko strain
Aedes aegypti	Bayer AG Monheim, Germany, via the Swedish University of Agricultural Sciences, Lund, Sweden, 2015	Rockefeller strain
Software and algorithms		
Methods S1	DRYAD repository as part of this paper	https://doi.org/10.5061/dryad.ttdz08m09
Matlab R2019b	Mathworks	https://www.mathworks.com/
MATJAGS, a Matlab interface for JAGS	Steyvers and Kalish[48]	https://github.com/msteyvers/matjags
JAGS 4.3.0 - Just Another Gibbs Sampler	JAGS	https://mcmc-jags.sourceforge.io
Matlab Toolbox for Bayesian Estimation (MBE)	Kruschke[49] Winter[50]	https://github.com/NilsWinter/matlab-bayesian-estimation; https://doi.org/10.1037/a0029146
Hidden Markov Model (HMM) Toolbox for Matlab.	Murphy[51]	https://www.cs.ubc.ca/~murphyk/Software/HMM/hmm.html

RESOURCE AVAILABILITY

Lead contact

Further information and requests for resources and reagents should be directed to and will be fulfilled by the lead contact, Florian T. Muijres (florian.muijres@wur.nl).

Materials availability

This study did not generate new unique reagents.

Data and code availability

- Three-dimensional tracking data and corresponding meta-data are publicly available as **Database S1** in the DRYAD repository https://doi.org/10.5061/dryad.ttdz08m09 (see key resources table).
- All original code is publicly available as **Methods S1** in the DRYAD repository https://doi.org/10.5061/dryad.ttdz08m09 (see key resources table).
- Any additional information required to reanalyze the data reported in this paper is available from the lead contact upon request.

EXPERIMENTAL MODEL AND SUBJECT DETAILS

Experimental animals

In our experiments, we used female *Anopheles coluzzii* and *Aedes aegypti* mosquitoes. *Anopheles coluzzii* mosquitoes came from a colony that originated from Suakoko, Liberia in 1987. The colony of *Aedes aegypti* mosquitoes (Rockefeller strain) was obtained via Bayer AG Monheim, Germany in 2015. Both colonies are housed in the Laboratory of Entomology (Wageningen University & Research, The Netherlands) with a shifted clock 12h light:12h dark cycle. Mosquitoes were reared at fixed temperature of 27°C and relative humidity of 70%. Adults were kept in BugDorm cages (30 × 30 × 30 cm, MegaView Science Co. Ltd., Taiwan). They had constant access to 6% glucose sugar water solution and were blood-fed daily with human blood (Sanquin, Nijmegen, The Netherlands) using a membrane feeding system (Hemotek, Discovery Workshop, UK). In the cages, female mosquitoes had access

to wet filter papers for egg-laying. Upon collection, eggs were dried for three days after which they were moved to plastic larval trays filled with 27°C water containing several drops of Liquifry No. 1 fish food (Interpet, UK). Emerging larvae were fed with TetraMin Baby (Tetra Ltd, UK). The handling of pupae differed slightly between the two species. *Anopheles* pupae were placed directly in new BugDorm cages to emerge, whereas *Aedes* pupae stayed in their larvae trays covered with nylon netting material. Twice a week, emerged *Aedes* adults were vacuumed to new BugDorm cages. Males and females were kept together so they could mate. Non-blood-fed adult females (age=7.6±2.3 days post-emergence, mean±standard deviation) were used in our experiments.

METHOD DETAILS

The flight arena

In this study, we filmed free flying mosquitoes in a custom-made octagonal flight arena (50×50×48 cm, height×width×length) with transparent Plexiglas walls (see Figure 1A). A visible light panel (20×48 cm) with 176 LEDs (Osram OSLON SSL 80°, CS8PM1.PM) was positioned above the flight arena. Multiple polyester neutral density filters of 0.8ND (LEE filters, Panavision Inc.) were used to stop down the light intensity of four LEDs to mimic twilight condition. Additionally, 4 infrared light panels (three panels of 20×48 cm and one panel of 50×50 cm) with a total of 600 LEDs (Osram OSLON Black Series (850 nm) 150°, SFH 4716A) were set around the flight-arena. The spectrums of the light conditions used in our experiments were measured and can be found in the Figure S2. Because mosquitoes cannot see infrared light,[52] the infrared light panels were used for backlighting flying mosquitoes. Mosquitoes could then be tracked in real time using Flydra (version 0.20.30)[53,54] and the live footage from 5 infrared-enhanced cameras (Basler acA2040-90umNIR). To each camera were attached one 12.5mm lens (Kowa LM12HC F1.4). A pixel-binning of 3 was used resulting in a recording resolution of 680x680 pixels and a framerate of 90 frames-per-second. Lens distortions were corrected using a backlighted print of a checkerboard pattern.[55]

To simulate an attacking threat, we build a swatter made of a 1 cm diameter black aluminium shaft and a transparent plexiglass disk with a diameter of 10 cm and a thickness of 1 cm, thus similar in size to a human hand. In order to vary the generated visual swatter cues, we covered the disk with either a clear or black mesh (Ornata plus 95135, howitec.nl, Figure S2). Here, we did not study this visual effect on the escape dynamics because it was outside the scope of the study.

The swatter (disk + shaft) was moved by a 50 cm long toothed-belt axes (drylin ZLW-1660-G0BW0-D0A3B-0A0A-500) powered by an AC servo motor (Schneider Electric Lexium BCH2 LD0433CA5C). The servo motor was controlled by a programmable motion servo driver (Schneider Electric Lexium LXM28A) programmed using the software SoMove 2 (Schneider Electric). The swatter kinematics (Figure 1E), was designed to have a peak velocity of around 1 m/s. This kinematic was based on preliminary experiments of human swatting hanging ping-pong balls and quantified data on mosquito flight speed that generally does not exceed 1 m/s.[22,56–58] The airflow velocity generated by the attack was quite similar to the one generated by an attacking bat.[31]

The temperature and relative humidity inside the experimental room were controlled by a previously described climate system.[58] To facilitate air circulation and cleaning inside the flight arena, there were circular holes in the front (diameter of 17.4 cm) and back (diameter of 43.7 cm) plexiglass panels. These holes were closed using easily removable high density polyethylene insect screenings (Howitec, The Netherlands). On the floor of the flight arena, we placed visual markers, randomly shaded grey squares printed on a plasticized paper sheet. Finally, a sensor recording local temperature and relative humidity (AM2302, ASAIR) was also placed inside the flight arena. Microcontroller boards (Arduino UNO) and custom-made scripts were used to communicate with the sensor, to trigger the swatter movement and to change the light condition from a nearby Linux computer. The setup was automated with the Robotic Operation System (ROS version Kinetic Kame).

Experimental procedure

In the late afternoon before each experimental day, the flight-arena was cleaned using a 15% ethanol solution and paper towels. Calibration was done by tracking a manually waved single LED inside the flight-arena. Then the new calibration was aligned to the flight arena coordinate system using a calibration device made of 8 LEDs positioned at various known three-dimensional locations. The flight arena was then closed. 50 female mosquitoes were transferred from a rearing cage to a release cage, which was then plugged to the side of the flight-arena. All handling of the mosquitoes and of the materials was done wearing nitrile gloves to avoid skin odour contamination. A dedicated Python 2.7 script was started to automatically run consecutive experiments with the different light conditions the succeeding day. By removing a metal mesh door, the mosquitoes could enter the flight arena and the experimenter left the room at 6 p.m. ± 1.2 h. The first experimental trial started 11.2 ± 3.0 h later the following morning.

Upon the start of the Python script controlling the experimental conditions, the light condition was set to follow the mosquito's normal light cycle in the rearing. Then the first experimental light condition was set, either at 2:30 a.m. for *Anopheles* mosquitoes (during their night phase) or at 8 a.m. for *Aedes* mosquitoes (during their day phase), in order to give mosquitoes two hours buffer time to adjust to their active phase. Three different light conditions were tested consecutively every day, each during an experimental window of 160 min. The order of these light conditions was changed following a quasi-randomized planning (see Table S1). The three light conditions tested for *Anopheles* mosquitoes were dark (visible light turned off), twilight and sunrise, whereas the ones for *Aedes* mosquitoes were twilight, sunrise, and overcast, resulting in an overlap of two light conditions between the two species (Figure 1G; Table S1). Neither *Anopheles* or *Aedes* were recorded flying in respectively overcast or dark because of their observed low flight activity in those light conditions.

Real-time estimations of mosquito positions and velocities were used to compute their predicted positions 367.5 ms in the future. Such latency corresponds to the time the swatter takes to be around halfway toward its most forward position. If the predicted position was found to be inside a sphere of interest, defined as a 10 cm diameter sphere in the centre of the flight arena, the swatter was triggered (Figure 1D). After one second, the swatter was moved back to its initial position and a delay of 10 seconds was respected before any new trigger of the swatter. During post-processing, mosquito initial positions and mean initial velocities (i.e. at trigger time) were used to filter out tracks that were not predicted to be inside the sphere of interest when the swatter would reach its most forward position. Thus, for the rest of the analysis, we only kept the tracks that were predicted to be entirely in the sphere of interest during the second half of the swatter movement (-157.5 to 0 ms).

When all the experiments of the day were finished, the experimenter came back into the room. A vacuum cleaner was plugged to the flight arena in place of the handling cage, and was used to capture all mosquitoes while avoiding potential escapes. The captured mosquitoes were left inside the vacuum cleaner to desiccate. Finally, the disk and mesh attached to the swatter rod were changed according to the previously mentioned plan (Table S1) for the next experimental day.

QUANTIFICATION AND STATISTICAL ANALYSIS

Analysis of three-dimensional flight tracks

Pre-processing was done using Python 2.7. For each trigger, collisions were manually identified by looking at the two-dimensional tracking results of the side cameras. A mosquito track with a collision was labelled as such when the tracked points of the swatter were intercepting the track. By projecting the swatter's three-dimensional shape into the two-dimensional view of each camera, the two-dimensional points of the swatter were filtered out for each trigger. The three-dimensional tracks of all mosquitoes were then reconstructed again, thus optimizing tracking performance near the swatter.

The rest of the analysis was done using Matlab R2019b. A first filtering of outlying three-dimensional points was done using the covariance matrices estimated by the extended Kalman filter used by the Flydra tracker. Then, less than four points long segments of mosquito tracks were filtered out, and segments that were separated by more than 15 missing points were divided in two different tracks. Remaining missing values were interpolated using the modified Akima piecewise cubic Hermite method (makima, Matlab). Then, in order to analyse only complete manoeuvres, we filtered out all the tracks that were not starting at least 60 frames before the most forward position of the swatter was reached (t = 0 s on Figures 2–7). Similarly, except for collisions, we filtered out tracks that ended less than 30 frames after the time when the swatter reached its most forward position. Finally, three-dimensional tracks were smoothed using a Savitzky-Golay filter with a moving window of five frames. Mosquito velocities and accelerations over time were computed using a second order derivate central finite difference scheme. Initial and final values were estimated respectively using forward and backward finite difference schemes. The angular flight speed was computed as in.[22] Then, the distance between the nearest point on the swatter disk was estimated using the synchronized position of the swatter over time (Figure 3A). The escape speed was defined and computed by projecting mosquito speed over time on the moving line between the nearest point on the swatter and mosquito three-dimensional position (see Figure 4A). The initial mean and standard deviation (std) of flight speed or angular speed was computed over the 11 frames around the frame at which the swatter was triggered. Finally, to see how much mosquitoes deviated from their initial trajectory, for each point in time we computed the Euclidian distance between their current position and the predicted position based on their initial position and initial mean velocity (Figure 3B). And the mean final Euclidian distance to predicted position of each mosquito was computed over the 11 frames around the frame at which the swatter reached its most forward position.

To be able to compare the chance of being hit by the swatter with or without potential mosquito responses (i.e. with the swatter on or off), collisions with a virtual swatter were predicted. These virtual collisions were estimated by computing if and when mosquito flight tracks would have crossed the path of the swatter (here virtual), assuming it had been triggered according to the triggering rules defined earlier.

Bayesian generalized linear model development

Here, we used several Bayesian generalized linear models (B-GLM) to model the flight behaviour and escape performance of mosquitoes. We used Bayesian statistics mainly because the Bayesian approach provides richer results than Frequentist statistics, by giving the probability distributions of the estimated parameters as well as an intuitive way of testing the null-hypothesis (see next paragraph). Additionally, in Bayesian statistics there is no need for multiple testing correction.[59,60] Also, we appreciate its conceptual clarity, whereas in Frequentist statistics there are common misconceptions about important concepts like *p-value*s and confidence intervals (e.g. interpreted as credibility intervals). Finally, in Bayesian statistics there is no need for multiple testing correction.[59,60]

In Bayesian statistics, before estimating the posterior distribution of a parameter mean (e.g. the slope of a statistical model), our prior knowledge of this distribution needs to be defined.[49] For this study, we had no prior knowledge of the standardized estimated mean parameters, therefore we used diffuse priors with a wide normal distribution (mean=0 and standard deviation=100). Then, the posterior distribution of the parameter is estimated by updating the prior distribution with new data (e.g. experimental results). This is computationally costly, and was done using Just Another Gibbs Sampler (JAGS) which use Markov chain Monte Carlo (MCMC).[61] Finally, null-hypothesis testing was done using the "HDI+ROPE decision rule,"[62] where the null-hypothesis is rejected if the 89% Highest Density Interval (HDI) of the standardized parameter is outside the Region of Practical Equivalence (ROPE = [-0.1, 0.1]). The 89% HDI being defined as the interval in which all the points have a higher probability density than points outside. The ROPE

is defined as the range around zero (i.e. the null-hypothesis) where, if estimated there, a parameter would be found to have ''practically no effect''. Thus, to reject the null-hypothesis, the HDI of an estimated parameter must fall outside the ROPE.

We estimated means of mosquitoes probability of being hit (Figure 2) for each combination of light condition and species using MATJAGS, a Matlab interface for JAGS,[48] and the Matlab Toolbox for Bayesian Estimation (MBE),[50] a Matlab implementation of Kruschke's R code.[49] To model the probability of being hit we used a Bernoulli distribution and a logistic link function. Then we compared the estimated mean distribution by computing standardized effect sizes. Here we defined the effect size between two groups as the difference of their means divided by the norm of their standard deviations.

For this study, we wrote a B-GLM package based on the two Matlab toolboxes previously mentioned MATJAGS,[48] and MBE.[50] JAGS modelling codes were based on examples from[63] and can be found in the **Methods S1** (and can be used with the **Database S1**). Binary response variables (like the probability of being hit P_{hit}) were modelled using Bernoulli distributions and a logistic link function. Flight metrics, like initial mean speed or mean angular speed, were modelled using gamma distributions and a log link function. To allow the use of the ''HDI+ROPE decision rule'', we standardized continuous predictors and response variable, by subtracting their mean and dividing them by two standard deviations (instead of one for typical z-scores).[64] All the other variables were binaries (e.g. was hit = yes/no), and they were only centred (i.e. to have zero mean). In this way, the estimated standardized slopes (i.e. effect sizes) are comparable across all models.[64,65]

B-GLMs were selected by applying a forward selection procedure, where compared models are increasingly complex by systematically including more predictors and their interactions. The best models were selected using the Akaike Information Criterion (AIC) and Bayesian Information Criterion (BIC). When comparing models of same complexity, we chose the model with the lowest AIC and BIC. When comparing models of different complexity, we selected a more complex model only if it had at the maximum an AIC and a BIC values 10 points inferior to less complex models.[63] Finally, we checked that good mixing of chains and low autocorrelation coefficients could be observed. A summary of all the B-GLMs that were compared to each other can be found in the **Data S1**.

Hidden Markov model development

For studying the escape manoeuvre dynamics of mosquitoes in response to a swatter attack, we developed a Hidden Markov model (HMM) using the Matlab toolbox by Kevin Murphy.[51] This HMM allowed us to determine in which of three behavioural escape flight states a mosquito was at each point in time, just by observing its escape velocity over time (Figure S3A). The probability of being in the states depending only on the previous state. The model was trained on all flight tracks recorded with the swatter on (i.e. without controls). The initial parameters of the model were found by fitting a mixture of three Gaussians to the distributions of all escape velocities of the tracks (fitgmdist, Matlab). Then a Baum–Welch algorithm, with fixed means and standard deviations, was used to find the unknown parameters of the HMM (see Figure S3). We labelled the first two states as ''cruising'' states toward or away from the swatter, and the last one as the ''escaping'' state (with high escape velocities away from the swatter, Figures S3A–S3D). The Viterbi algorithm was used to compute the most-likely corresponding sequence of states (see the example on Figure S3A). Almost all mosquitoes were found to initially be in one of the two cruising states (Figure S3). When the swatter started to move towards the centre of the flight arena, the proportion of mosquitoes in the cruising state away from the swatter grew. Then, around the time when the swatter was halfway towards its most forward position (t=0 s), mosquitoes started to get into the fast escape state. The maximum proportion of mosquitoes to be in this state over time was 17.1% and this maximum was reached just before the swatter arrived at its most forward position (Figure S3G). In the rest of the analysis, all the tracks that were predicted at least once to be in this fast escape state were labelled as fast escapes. In this way, each track was put in one of three groups, the collisions, the slow escapes and the fast escapes. The probability that a virtual swatter triggered a fast escape was lower than 1%, showing that the Hidden Markov Model produced practically no false positive fast escapes (Figure S3C). In contrast, probability that a real swatter triggered a fast escape was 20%. Because many flights do not get close to the swatter (Figures 3C and 3F), these percentages are not surprising.

Analysing the escape performance of mosquitoes

Using a combined statistical and mechanistic modelling of the mosquito flight dynamics, we studied how the two mosquito species adjust their flight dynamics to optimize their escape performance. We did this in four steps. First, we determined how the chance of being (virtually) hit by the swatter differed between species, light conditions, and swatter mode (on/off). Second, we studied how baseline protean flight behaviour affected the chance of being hit by the swatter. Third, we determined how the swatter-induced escape manoeuvre dynamics affected escape performance. Finally, we quantified the relative contributions of baseline protean behaviour and escape manoeuvre dynamics (protean and systematic) to the overall escape performance.

Modelling the chance of being hit by the swatter

In our first sub-study, we estimated the probability of being hit P_{hit} by determining in all flight tracks whether the mosquito was hit. Based on these data, we used a B-GLM to model the probability of being hit P_{hit} as a function of the experimental conditions (Figure 2), with the following predictors: swatter off or on (0 or 1), species (*Anopheles* or *Aedes*), logarithm of light condition luminance (cd/m^2), reference (dark for *Anopheles* or overcast for *Aedes*) or altered light (twilight and sunrise), mesh colour (black or clear), time after start of first trial, humidity, and temperature. In addition, to test for learning effect, we also used the interaction between the two following predictors: swatter on/off and the time after start of first trial. Finally, in order to check for potential behavioural difference of the two species, and if the predictor species was already in the model, we compared models with interactions between *Anopheles* or *Aedes* with the other remaining predictors (e.g. *Anopheles*.*time to test if *Anopheles* mosquitoes' behaviour was changing over time). The final set of predictors included in the minimal model were swatter off or on, species, and the interaction *Anopheles**light condition

(altered or reference). To improve clarity and because it didn't change the results, we added the interaction *Aedes**light condition to the model shown in Figure 2.

Modelling the baseline protean flight behavior

We studied how baseline protean flight behaviour affected the escape performance using two steps. First, we used a B-GLM to model how P_{hit} varied in function of the initial flight state of the mosquito. The minimum B-GLM was determined by using the mean or standard deviation of the initial linear flight speed or angular speed as predictors (Figures 4B, 4C, 4E, and 4F). Then, we modelled how the predictors left in the minimal model (initial mean of the speed and angular speed) changed with the experimental conditions while the swatter was off, using the same predictors as the ones used for initially modelling of P_{hit}. Note that for the case with the swatter off, the escape performance is only determined by the baseline protean behaviour, because without the swatter on no escape responses are elicited.

Studying the escape manoeuvre dynamics

In our third sub-study, we studied how the swatter-induced escape manoeuvres affected escape performance. We first used the Hidden Markov model to identify all rapid escape manoeuvres in all flight tracks. Then, we modelled with a B-GLM how the probability of performing a fast escape P_{escape} depended on the experimental conditions (Figure 6). The minimum model was determined using the same initial predictors as the ones used for modelling P_{hit}. We observed high autocorrelation and bad mixing of chains with the predictor swatter on or off, most likely because the number of fast escapes was really low during the controls. Thus it was decided to model P_{escape} separately for the tracks recorded while the swatter was triggered (Figures 6E–6J).

Modelling the contribution of escape strategies

In our forth sub-study, we tested how baseline protean flight behaviour and escape manoeuvre dynamics combined affected the escape performance. For this, we used the flight path deviation at t=0 s (d_0), because this parameter is an important metric for predicting escape performance. We did this in two steps.

First, we used a B-GLM to model the mean flight path deviation d_0 as a function of the experimental conditions (Figures 7D–7I). To get the minimal model, we used the same initial predictors as the ones previously described for the B-GLMs of P_{hit} and P_{escape}. The predictors included in the minimal model were the same as for the first B-GLM.

Secondly, we used the flight path deviation d_0 to quantify the relative contributions of baseline protean flight behaviour and escape manoeuvrability on the escape performance. For this we defined the relative baseline protean contribution to flight path deviations as $R_{protean}=d_{off}/d_{on}\cdot 100\%$ (Figures 7J–7L), where d_{off} and d_{on} are the flight path deviations at t=0 s when the swatter was turned off and on, respectively. Note that d_{off} is the result of only the baseline protean behaviour, and d_{on} is the result of the protean flight behaviour and the escape manoeuvre combined. Thus, $R_{protean}$=100% if a flight path deviation is fully caused by the baseline protean behaviour, and $R_{protean}$=0% when a flight path deviation is fully caused by the escape manoeuvre. Using a Bayesian model, we estimated means of $R_{protean}$ for each combination of light condition and species (Figures 7J and 7K).[49] To model $R_{protean}$ we used a log-normal distribution and estimated the means each combination from a sample of 10,000 randomly chosen values of $R_{protean}$ out of all the computed $R_{protean}$ values. Then we compared the estimated mean distribution by computing standardized effect sizes.